

ORIGINAL ARTICLE

Comparison of different X-ray-based scanning electron microscopy methods to detect sub-nanometre ultra-thin InAs layers deposited on top of GaAs

Thomas Walther¹  | Stuart Creasey-Gray² | Stephan Boehm³ | Heath Young³ | Yang Yang³

¹School of Electrical and Electronic Engineering, University of Sheffield, Sheffield, UK

²Sorby Centre for Electron Microscopy, Kroto Research Institute, North Campus, University of Sheffield, Broad Lane, UK

³Bruker Nano Analytics, Am Studio 2D, 12489 Berlin, Germany

Correspondence

Thomas Walther, School of Electrical and Electronic Engineering, University of Sheffield, Mappin St, Sheffield S1 3JD, UK.
Email: t.walther@sheffield.ac.uk

Abstract

We compare three different methods of X-ray analysis in a scanning electron microscope (SEM): energy-dispersive X-ray spectroscopy (EDX), wavelength-dispersive X-ray spectroscopy (WDX) and micro X-ray fluorescence (μ XRF). These methods are all applied to the same gallium arsenide (GaAs) wafer with a 0.8 nm layer of indium arsenide (InAs) on top. All methods allow detection and quantification of the indium L-line intensity from the thin InAs layer. EDX is the easiest to perform, WDX is the most sensitive and μ XRF a novel technique where a poly-capillary optics is used to focus an X-ray beam from a high-voltage X-ray tube onto a small spot several micrometres wide and the characteristic X-rays produced are detected by a solid-state silicon detector similar to that used in EDX. It is to our knowledge the first time a sub-nanometre layer is reliably detected and analysed using μ XRF in an SEM.

KEYWORDS

detection limit, energy-dispersive X-ray spectroscopy (EDX), indium gallium arsenide (InGaAs), micro X-ray fluorescence (μ XRF), sensitivity, wavelength-dispersive X-ray spectroscopy (WDX)

1 | INTRODUCTION

Surface analysis of thin films can be achieved by different techniques where those that yield ultra-low (parts-per-million, ppm) sensitivity often have low penetration (e.g. secondary ion mass spectroscopy, SIMS) or low escape depths (e.g. Auger electron spectroscopy, AES) and so typically need to be combined with destructive depth profiling^{1,2} while those with high penetration (e.g. proton-induced X-ray generation, medium energy ion scattering)³ are often hard to quantify. X-ray photoelectron spectroscopy (XPS) lies somewhere in-between but usually

does not yield any lateral resolution as would be needed for characterising laterally inhomogeneous systems.

Techniques that rely on X-ray generation and detection and can be incorporated into a scanning electron microscope (SEM) to yield non-destructive compositional mapping across surfaces with a lateral sub- μ m-scale resolution include energy-dispersive X-ray spectroscopy (EDX), wavelength-dispersive X-ray spectroscopy (WDX) and micro X-ray fluorescence spectroscopy (μ XRF). Of course, scanning AES and nanoSIMS can also achieve chemical mapping with sub- μ m lateral resolution but require rather specialised instrumentation that is not

This is an open access article under the terms of the [Creative Commons Attribution](https://creativecommons.org/licenses/by/4.0/) License, which permits use, distribution and reproduction in any medium, provided the original work is properly cited.

© 2025 The Author(s). *Journal of Microscopy* published by John Wiley & Sons Ltd on behalf of Royal Microscopical Society.

available in most laboratories (and neither at University of Sheffield).

SEM-EDX has been shown to be sensitive in the few at. % range,⁴ while SEM-WDX⁵ and μ XRF^{6,7} can both reach 10 ppm level sensitivity for heavy elements.

For very thin surface layers on bulk substrates the penetration depth of the electrons and the interaction volume for X-ray generation will always be much larger than the layer thickness so quantification in top-down geometry is tricky. A previous top-down investigation of several thin In(Ga)As layers grown on GaAs has been able to detect indium in various In(Ga)As layers as thin as an individual unit cell even in a simple Hitachi 3030+ tabletop SEM with tungsten filament and 30 mm² Bruker XFlash 430 SDD (15 kV, ~1 h acquisition time).⁸ We have previously checked the appropriateness of In L/As L X-ray line ratios for quantification of EDX with the help of an InAs wafer sample, which is not discussed here but in detail in Ref. (8). For InAs bulk where absorption in the sample is dominant, experiment and simulation differ systematically by 7%–8% if the differences between the detector windows used in our SEM-EDX experiment (ultrathin window of type Moxtek AP3.3) and in simulations (thicker Al coating but thinner parylene polymer) are taken into account.

Here we compare quantification of EDX at 5 or 15 kV in this instrument to WDX in a dedicated JEOL JXA 8530F+ electron microprobe equipped with four crystal spectrometers using Rowland circle geometry and operated at 5 kV where beam current is more than an order of magnitude higher and the penetration depth smaller. Finally, for μ XRF a Quantax X Trace 2 system with an X-ray tube with Rh target⁹ has been used where penetration at higher voltage of 25–50 kV will be an order of magnitude deeper. Our study builds on a more theoretical comparison of WDX and μ XRF methods reported earlier by Procop and Hodoroba¹⁰ who assessed the quantifiability of the latter by modelling analytically photo-ionisation cross-sections, Bremsstrahlung and characteristic X-ray intensities for K- and L-lines in XRF. Our contribution is an experimental comparison of detection and sensitivity limits of three SEM-based techniques applied to an InGaAs semiconductor wafer. Such samples are relevant for optoelectronics as thin strained InAs layers deposited on GaAs(001) can relax some of the compressive strain by spontaneous quantum dot formation on the surface and simultaneous segregation and interdiffusion.^{11,12}

2 | SIMULATIONS

Figure 1 shows results from Monte–Carlo simulations of electron scattering and X-ray generation and detection using the CASINO software v2.42.¹³ While 5 kV accelera-

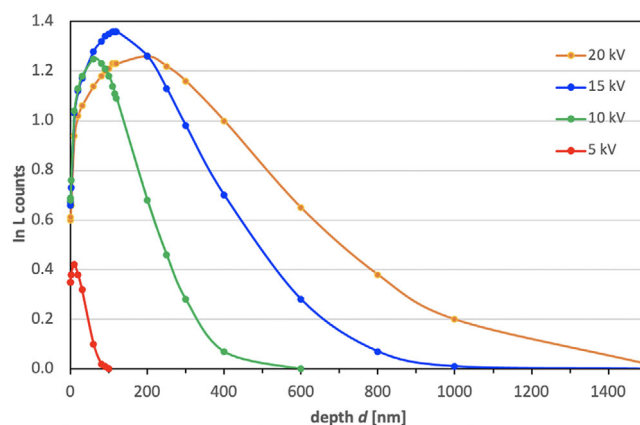


FIGURE 1 Simulation of number of In L counts produced from a 1 nm thin InAs layer embedded in GaAs as function of depth below the surface for different acceleration voltages for a nominal take off-angle (ToA) of 25°.

tion voltage will produce In L counts preferentially near the surface, which should be beneficial for thin surface layer detection, the absolute number of counts produced is low because the over-voltage is only slightly above that required to produce In L X-rays, all of which lie in the 3.3–3.9 keV range. For 10–20 kV, electron penetration and X-ray generation volume both increase with acceleration voltage but the number of In L X-rays produced near the surface is almost constant and about twice as high as at 5 kV. For EDX, 15 kV is therefore a good compromise between sufficient X-ray production yield and penetration while for WDX, where the background is lower and the signal-to-noise ratio thus better, 5 kV may be a better choice.

3 | EXPERIMENTS

Below, we will correlate measurements of the same wafer sample by EDX, WDX and μ XRF in different scanning electron microscopes. Wafer pieces were investigated in top-down geometry without any specimen preparation apart from cleaning with HPLC-grade acetone (99.9% pure, Sigma-Aldrich, Burlington, MA).

The indium signal from the In L β line coincides with the position of possible sum peaks from Si K (see Figure 2), which, together with the high Bremsstrahlung background, ultimately limits the detection of very small amounts of indium in EDX. The In L α line is barely visible upon the background in EDX at 5 kV acceleration voltage (cf. Figure 3). It is clearly visible at 15 kV, the In L β being only marginally detectable. So, in agreement with the previous study⁸ we evaluate the In_L/As_L ratio at 15 kV, the longer acquisition time of ~2 h used here giving us a

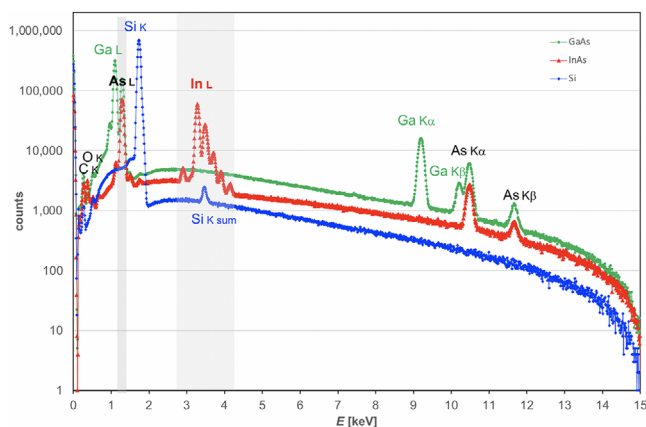


FIGURE 2 Experimental EDX spectra of GaAs, InAs and Si reference samples at 15 kV. Relevant peaks are labelled. ToA of 22°.

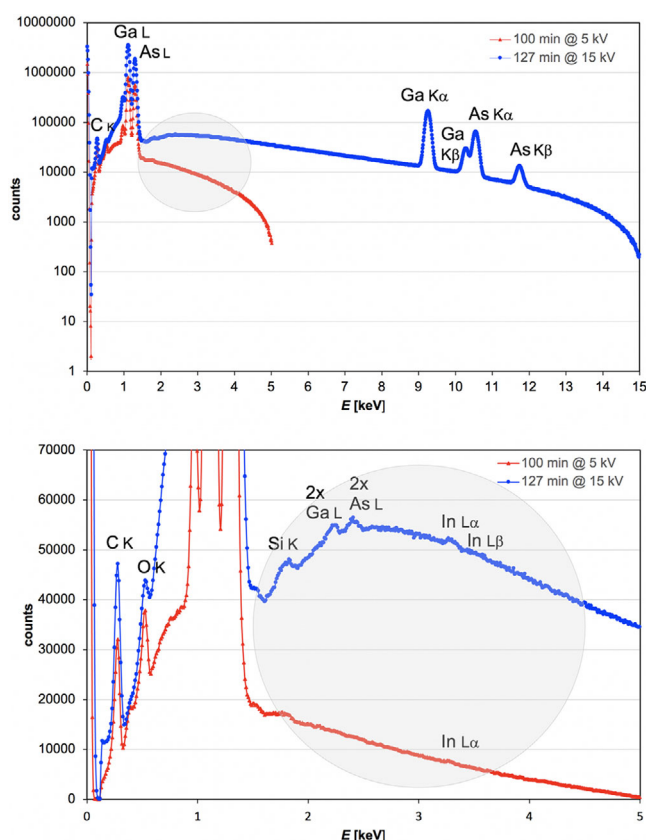


FIGURE 3 EDX spectra on log scale (above) and on shrunk linear scale (below) of EDX spectra of InAs-on-GaAs sample AF9151 at 5 kV (lifetime: 49 min, 1.4% deadtime) and 15 kV (lifetime: 113 min, 11.3% deadtime). Relevant peaks are labelled where the prefix 2x refers to (weak) sum peaks. ToA of 22°.

slightly improved detection limit. Numbers given in the following are net intensities after background subtraction from the 15 kV spectra shown in Figure 3, as measured by Bruker's Quantax 70 software. From the count ratio $In_L/As_L = (24,239 \pm 5000)/(13,581,340 \pm 7000) = 1.78 \pm 0.37 \text{‰}$, we get $0.88 \pm 0.18 \text{ nm}$ or $2.9 \pm 0.6 \text{ ML}$ equivalent of

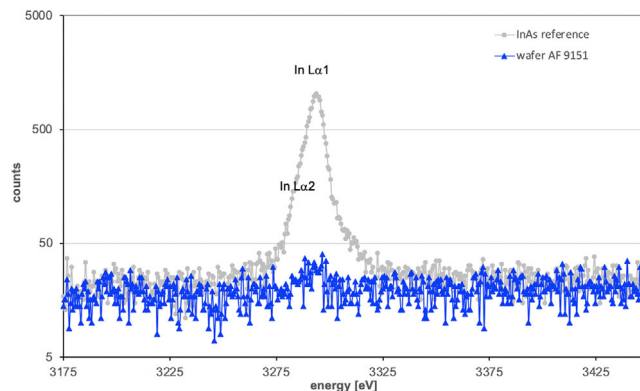


FIGURE 4 WDX spectra of In L taken at 5 keV of an InAs reference sample (grey) and the InAs-on-GaAs sample AF9151 (blue) recorded on channel 4 using a PET-L detector, displayed on log scale. The In L peak counts of ~1000 for InAs and 29 for InAs-on-GaAs are the results from 4s integration. As L and Ga L signals were recorded simultaneously using additional TAP and TAP-H analyser crystals, respectively. Total recording time was 33 min for each of two scans, one using a 2 μm and the other a 4 μm large probe. ToA of 40°.

InAs, where the error bar is a little smaller than previously reported ($2.7 \pm 0.8 \text{ ML}$) due to doubling of the acquisition time and a little increase in beam current, however, the error bar will ultimately be limited by background fitting at this stage and will likely not reach what WDX can achieve (see below). A monolayer (ML) equivalent is another way to express the chemical width a very thin layer, by multiplying its physical width in monolayers (here: single group-III metal layers in the sphalerite lattice, spaced a distance $a/2$ along the [001] growth direction) with the fractional chemical occupancy of that layer: one complete atomic layer would give the same chemical signal as n layers wherein only $(1/n)^{\text{th}}$ of each was occupied by the atomic species in question. A unit cell of InAs is 0.60 nm thick and thus would make up 2 ML equiv. of indium and 2 ML equiv. of arsenic.

Quantification of the complete WDX spectra for In L (shown in Figure 4) and As L, scanning a 2 μm or a 4 μm large defocused 5 keV electron beam with 15 nA current over the surface of sample AF9151, gave indium weight percentages of $0.52 \pm 10 \text{ wt\%}$ and $0.44 \pm 0.05 \text{ wt\%}$, respectively, whose weighted average would be $0.46 \pm 0.04 \text{ wt\%}$. Taking the different atomic weights of Ga, As and In into account, this would mean $0.29 \pm 0.02 \text{ at. \%}$ indium for an ideal $In_xGa_{1-x}As$ alloy, that is, $x = 0.0058 \pm 0.0005$. Comparing again CASINO Monte-Carlo simulations of both an $In_{0.0058}Ga_{0.9942}As$ bulk with a thin pure InAs film (density $\rho = 5.68 \text{ g/cm}^3$) on GaAs bulk (substrate, density $\rho = 5.32 \text{ g/cm}^3$) imaged at 5 kV, a 40° take-off angle would suggest both to give ratios of $In_L/As_L = 1.15\text{‰}$ and $In_L/Ga_L = 0.93\text{‰}$ for an InAs film thickness of

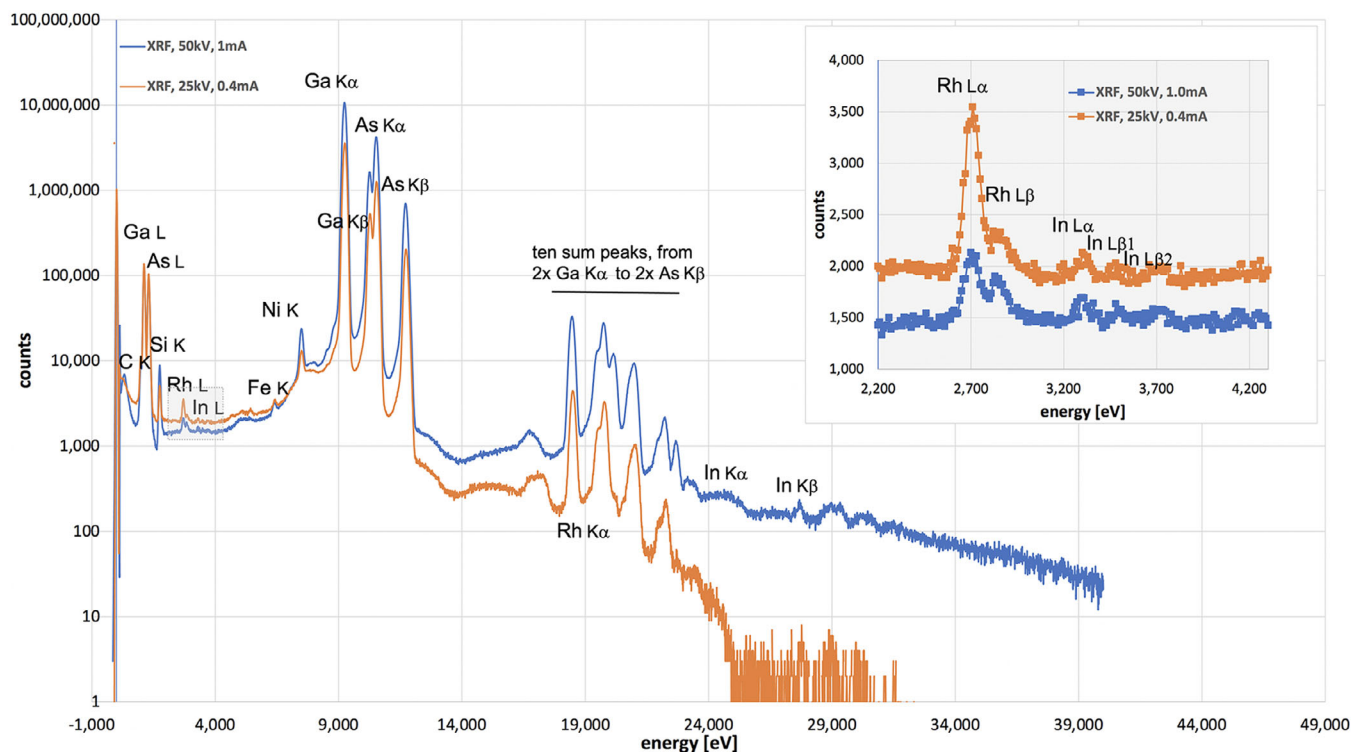


FIGURE 5 Micro-XRF spectra of InAs-on-GaAs sample AF9151 at 25 kV (with a 60 mm² SDD) and 50 kV (with a 30 mm² SDD). The area of 2.2–4.2 keV around the Rh L and In L lines is shown enlarged in the top right. Acquisition time for 50 kV: 76 min total, 58 min live time.

0.78 ± 0.10 nm. Using the lattice parameter of $a_{\text{InAs}} = 0.606$ nm, which corresponds to 2 d_{002} monolayers (ML), WDX quantification finally yields 2.5 ± 0.3 ML equivalent of pure InAs.

Micro X-ray fluorescence (μ XRF) has been measured in a SEM with Quantax X Trace 2 using a poly-capillary X-ray optics coupled with a Rh target. The SEM functionality was only used for navigation and focusing. In the μ XRF spectra in Figure 5, one can see that detection of the In L signal interferes with the Rh L signal from the X-ray source, which could be suppressed by a thin aluminium foil as filter commonly applied at the exit of the X-ray tube to avoid diffraction (but wasn't used here). In K signals at 24–28 keV cannot be generated by 25 kV electrons or X-rays at all, and stay weak even at 50 kV electron acceleration voltage, but the In L signals from the $L\alpha$, $L\beta_1$ and $L\beta_2$ sub-lines are all well visible. Their integrated net signal amounts to about 1400 counts here. Their quantification, however, is difficult. The InL/AsL and InL/GaL line intensity ratios of 2.15‰ and 1.46‰ measured at 50 kV are similar to what EDX and WDX observe. Full quantification necessitates, however, a comparison with either experimental XRF spectra from pure elements or calculated standards taken at the same acceleration voltage. For 50 kV, Bruker uses a database for a 60 mm² SDD with experimental intensities for the Ga K-line from a metallic gallium standard and for the In L-line an interpolated value for metallic

indium. Correcting for the different densities between metals used as standards and semiconductors measured here, taking into account the smaller SDD used for the 50 kV measurement as well as the acquisition live time, gives an estimate of the indium thickness on the surface of 0.8 nm, with a relative error of up to 25%, corresponding to 0.8 ± 0.2 nm, or 2.6 ± 0.7 ML equivalent of pure InAs. This value lies between the earlier results from EDX and WDX, and error bars overlap.

4 | CONCLUSION

EDX, WDX and μ XRF in an SEM are all able to detect a 0.8 nm thin InAs on a GaAs(001) wafer, and quantification results are consistent within the error bars. The sensitivity is best in WDX because of its low background signal. EDX has a worse sensitivity due to the high bremsstrahlung background, which makes detecting tiny peaks on top difficult. To the authors' knowledge this is the first time a sub-nm surface layer has been reliably detected and quantified by μ XRF in an SEM.

The absolute quantification errors are small, with standard RMS errors for EDX and μ XRF of 0.6–0.7 ML equivalent (and half of that for WDX) while the relative errors are large because they are limited by both intrinsically poor counting statistics from very thin surface layers

as well as systematic errors due to background subtraction (EDX only) and the reliability of the reference material standards because of the unavoidable slight surface oxidation of compound semiconductors as well as pure metals (used for μ XRF).

Regarding practical implementation, this study strengthens the case for using SEM-EDX despite its lowest sensitivity, as this is a method commonly found in industrial and research cleanrooms, while WDX and μ XRF are more elaborate techniques not normally used in cleanrooms environments. If one used a field emission SEM with higher beam current than the tungsten filament in our tabletop SEM then similar experiments could be conducted within ~ 10 – 15 min rather than 2 h, making them useful for quality control and feedback during growth and device processing.

Our comparison of the surface analysis capability of three imaging methods based on scanning electron microscopes has here only been performed for one type of material but should be extendable to all types of single layers that contain at least one chemical element that produces detectable X-rays above 100 eV (i.e. not H, He or Li) and does not occur in the underlying substrate. For native oxide layers on silicon wafers one of the authors has already shown that SEM-EDX yields sub-nm sensitivity and high accuracy.¹⁴ A transfer to multilayers, however, would only be possible under very specific additional conditions regarding their chemistry and repetition that would require detailed modelling.

ORCID

Thomas Walther  <https://orcid.org/0000-0003-3571-6263>

REFERENCES

- Hantsche, H. (1989). Comparison of basic principles of the surface-specific analytical methods: AES/SAM, ESCA (XPS), SIMS, and ISS with X-ray microanalysis, and some applications in research and industry. *Scanning*, *11*, 257–280.
- Knorsch, M., Nadoll, P., & Klemd, R. (2020). Trace elements and textures of hydrothermal sphalerite and pyrite in Upper Permian (Zechstein) carbonates of the North German Basin. *Journal of Geochemical Exploration*, *209*, 106416.
- Campbell, J. L., Teesdale, W. J., & Halden, N. M. (1995). Theory, practice and application of PIXE microanalysis and SPM element mapping. *Canadian Mineralogist*, *33*(2), 279–292.
- Newbury, D. E., & Ritchie, N. W. M. (2019). Electron-excited X-ray microanalysis by energy dispersive spectrometry at 50: Analytical accuracy, precision, trace sensitivity, and quantitative compositional mapping. *Microscopy and Microanalysis*, *25*(5), 1075–1105.
- Batanova, V. G., Sobolev, A. V., & Magnin, V. (2018). Trace element analysis by EPMA in geosciences: Detection limit, precision and accuracy. *IOP Conference Series: Materials Science and Engineering*, *304*, 012001.
- Davis, J. M., Newbury, D. E., Fahey, A., Ritchie, N. W. M., Vicenzi, E., & Bentz, D. (2011). Bridging the micro-to-macro gap: A new application for micro X-ray fluorescence. *Microscopy and Microanalysis*, *17*(3), 410–417.
- Haschke, M., & Boehm, S. (2017). Chapter 1: Micro-XRF in scanning electron microscopes. *Advances in Imaging and Electron Physics*, *199*, 1–60. DOI: [10.1016/bs.aiep.2017.01.001](https://doi.org/10.1016/bs.aiep.2017.01.001)
- Walther, T. (2022). Measuring non-destructively the total indium content and its lateral distribution in very thin single layers or quantum dots deposited onto gallium arsenide substrates using energy-dispersive X-ray spectroscopy in a scanning electron microscope. *Nanomaterials*, *12*(13), 2220.
- Bruker (2025). Electron Microscope Analyzers QUANTAX micro-XRF. available at: <https://www.bruker.com/en/products-and-solutions/elemental-analyzers/eds-wds-ebisd-SEM-Micro-XRF/quantax-micro-xrf.html> (accessed 18 November 2025)
- Procop, M., & Hodoroaba, V. D. (2008). X-ray fluorescence as an additional analytical method for a scanning electron microscope. *Microchimica Acta*, *161*(3–4), 413–419.
- Walther, T., Cullis, A. G., Norris, D. J., & Hopkinson, M. (2001). Nature of the Stranski-Krastanow transition during epitaxy of InGaAs on GaAs. *Physical Review Letter*, *86*(11), 2381–2384.
- Walther, T. (2022). Role of interdiffusion and segregation during the life of indium gallium arsenide quantum dots, from cradle to grave. *Nanomaterials*, *12*(21), 3850.
- Drouin, D., Real Couture, A., Joly, D., Tastet, X., Aimez, V., & Gauvin, R. (2007). CASINO V2.42—A fast and easy-to-use modeling tool for scanning electron microscopy and microanalysis users. *Scanning*, *29*, 92–101.
- Walther, T. (2021). Measurement of nanometre-scale gate oxide thicknesses by energy-dispersive X-ray spectroscopy in a scanning electron microscope combined with Monte Carlo simulations. *Nanomaterials*, *11*(8), 2217.

How to cite this article: Walther, T., Creasey-Gray, S., Boehm, S., Young, H., & Yang, Y. (2025). Comparison of different X-ray-based scanning electron microscopy methods to detect sub-nanometre ultra-thin InAs layers deposited on top of GaAs. *Journal of Microscopy*, 1–5. <https://doi.org/10.1111/jmi.70049>